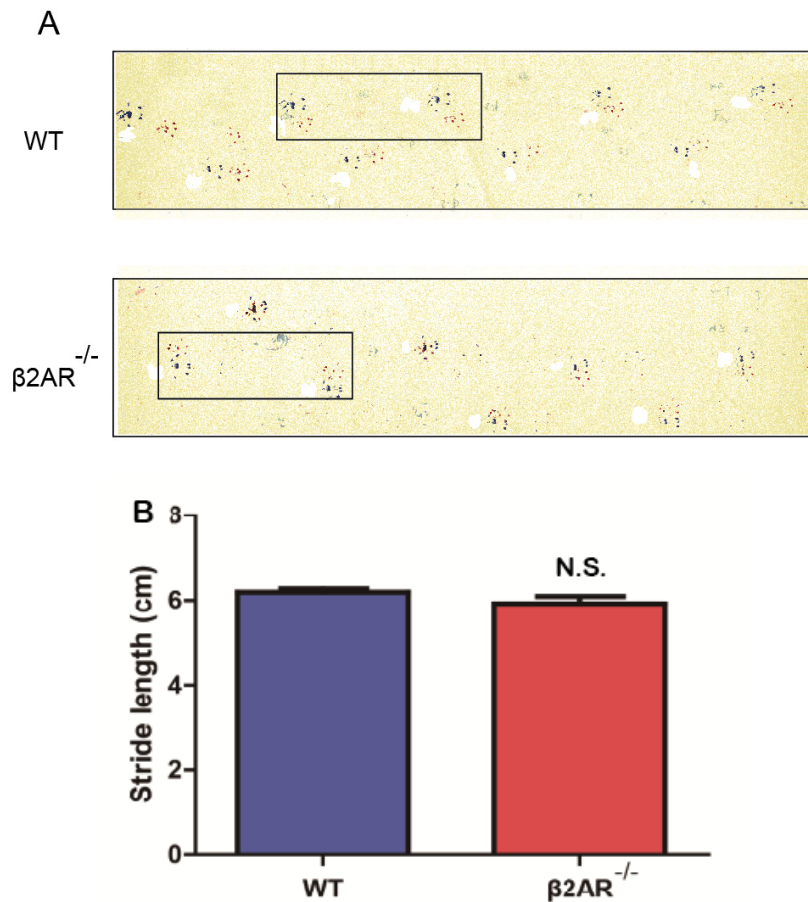


## Adaptive Activation of a Stress Response Pathway Improves Learning and Memory Through Gs and $\beta$ -arrestin-1 Regulated Lactate Metabolism

### Supplemental Information

#### Supplemental Figures



**Fig. S1. Compared to their wild-type littermates, the  $\beta 2AR^{-/-}$  mice show no motor impairment in the footstep test.**

The  $\beta 2AR^{-/-}$  mice (n=10) and their wild-type littermates (n=10) were trained for 5 days before testing. The results show that there were no significant differences between the  $\beta 2AR^{-/-}$  mice and their wild-type littermates in their movement ability. The red footsteps are the mouse's forelimb, and the blue ones are the hind limb. (A) Representative images of the footstep test; (B) Statistical analysis and bar graph representation of (A).

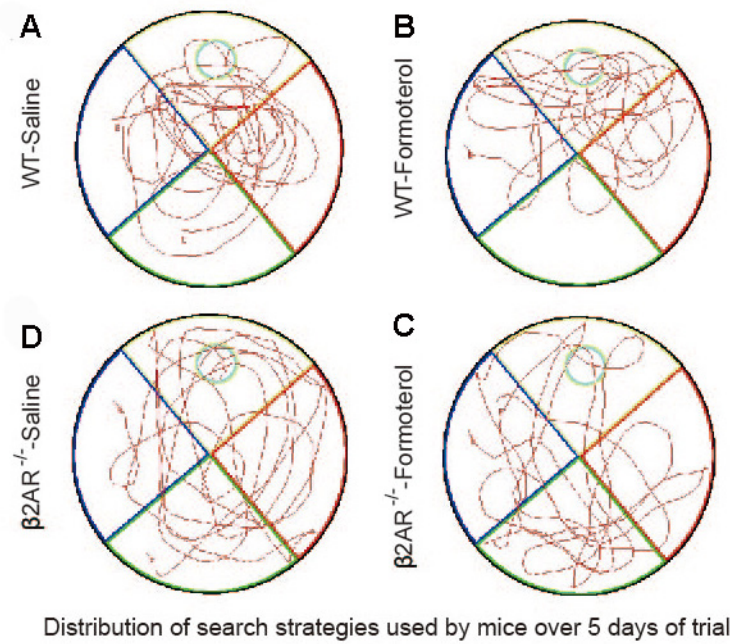


**Fig. S2. Distribution of searching strategies used by WT and  $\beta 2AR^{-/-}$  mice over 5 days of trials.**

Typical swim-tracking path employed by WT mice treated with saline (A); WT mice treated with formoterol (B);  $\beta 2AR^{-/-}$  mice treated with saline (D); and  $\beta 2AR^{-/-}$  mice treated with formoterol (C).

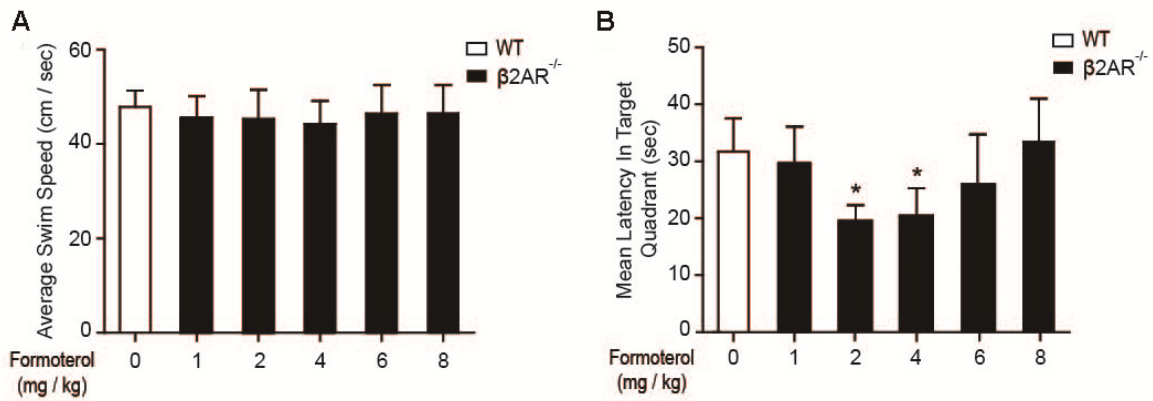


**Fig. S3. Dose response of formoterol in MWM experiments.**

The C57 WT mice were randomly divided into six groups and received injections of either formoterol (0, 1, 2, 4, 6, 8 mg/kg) or saline 4 h for five days before behavioral tests. Results indicated there was no variation in the average swimming speed of the mice ( $n = 20$ ) between different groups (A). However, the mean escape latencies of WT mice that were administered 2 or 4 mg/kg formoterol were significantly shorter than that of WT mice treated with saline. The formoterol-treated group were compared with saline-treated group (\*,  $P=0.0416$ ,  $P=0.0482$ ).

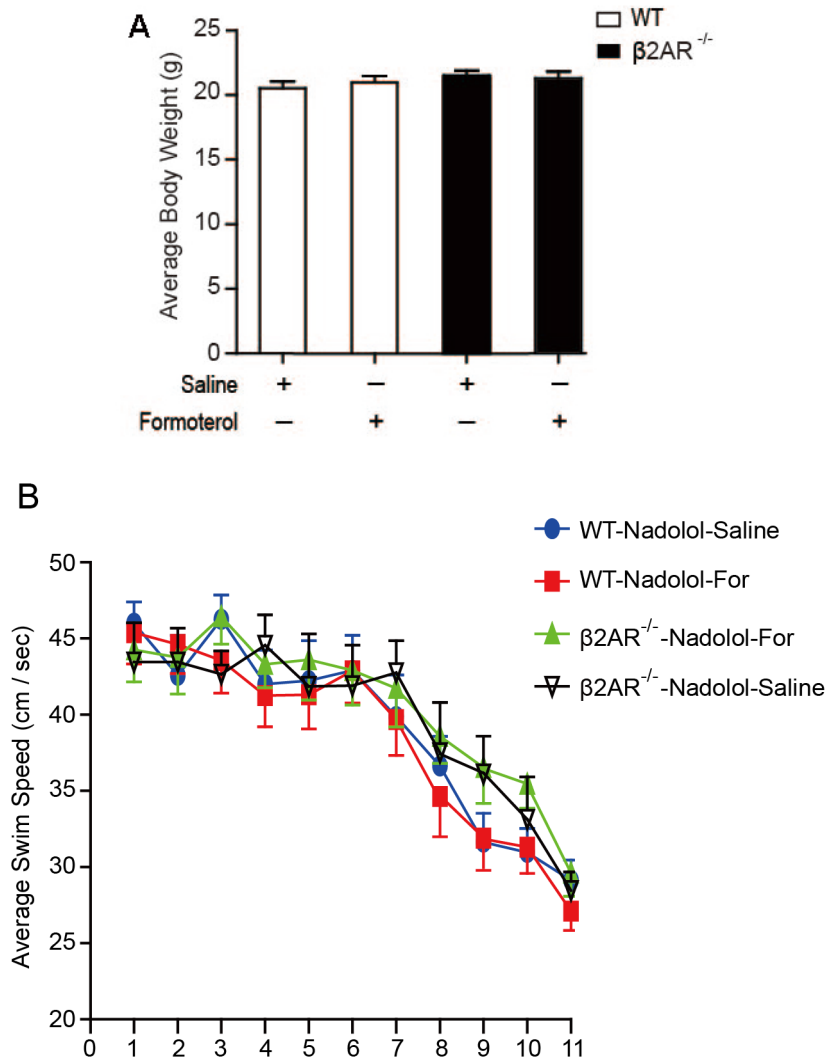


**Fig. S4. Supplemental information for MWM experiments in Figure 1.**

The C57 WT mice and  $\beta 2AR^{-/-}$  mice were randomly divided into two groups and received injections of either formoterol (2 mg/kg) or saline 4 h before behavioral tests; body weight (A) and swimming speed (cm/sec) (B) were measured. Results indicated there were no significant differences in body weight between each group. There were no significant differences in the average swimming speed between the different groups of mice (n = 20).

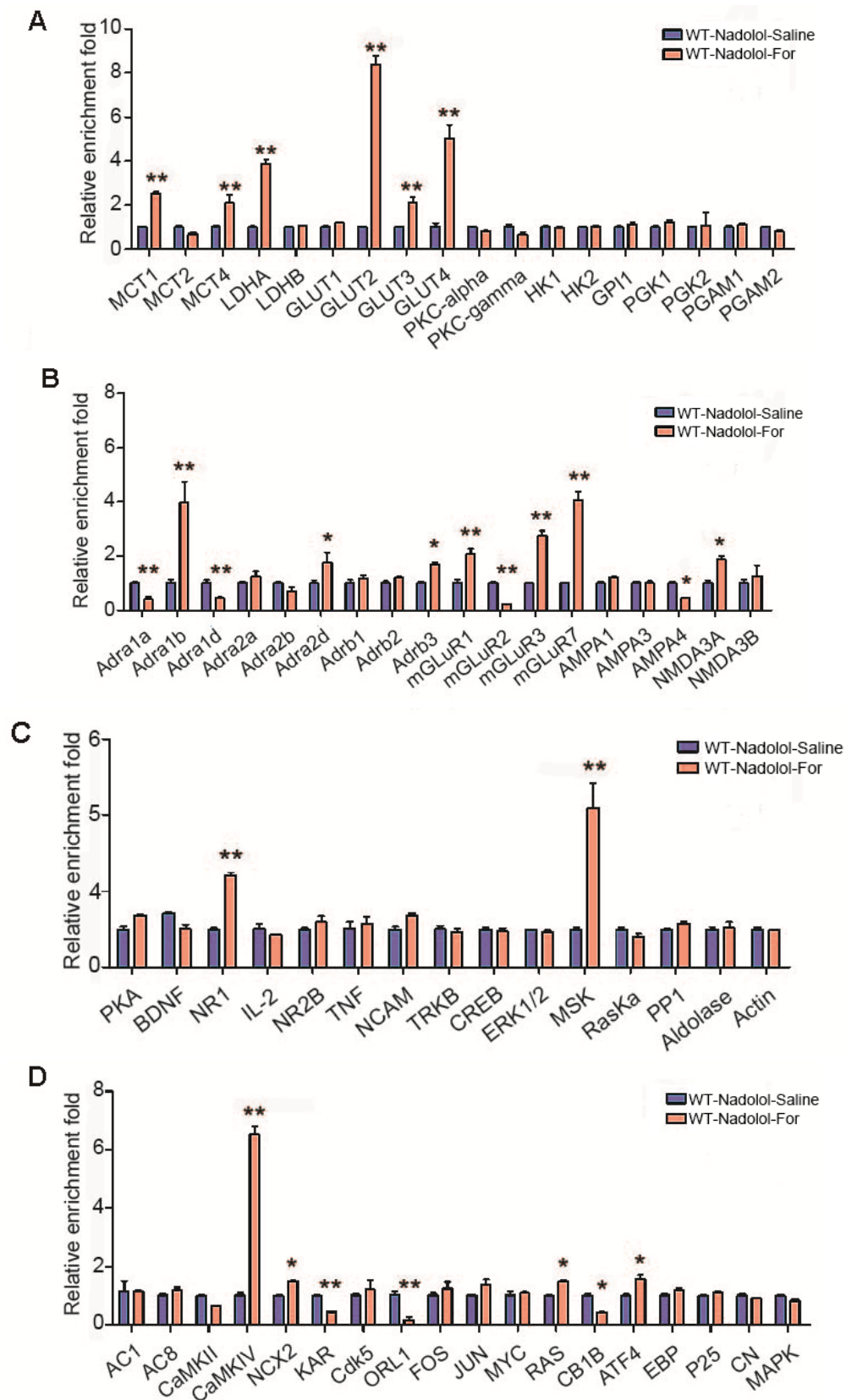


**Fig. S5. Quantitative RT-PCR (QRT-PCR) analysis of mRNA transcription profiles of genes important for learning and memory after formoterol stimulation.**

Expression levels were normalized with actin levels. Wild type mice were administrated with formoterol for 3 days and the hippocampus were dissected for QRT-PCR analysis. 6 mice

were used for each group. \*,  $P < 0.05$ ; \*\*,  $P < 0.01$ , mice administered formoterol were compared with those administered saline. MCT4, monocarboxylate transporter 4; MCT2, monocarboxylate transporter 2; MCT1, monocarboxylate transporter 1; LDHA, lactate dehydrogenase A; LDHB, lactate dehydrogenase B; GLUT1, glucose transporter 1; GLUT2, glucose transporter 2; GLUT3, glucose transporter 3; GLUT4, glucose transporter 4; PKC-gamma, protein kinase C, gamma; PKC-alpha, protein kinase C, alpha; HK1, hexokinase 1; HK2, hexokinase 2; GPI1, glucose phosphate isomerase 1; PGK1, phosphoglycerate kinase 1; PGK2, phosphoglycerate kinase 2; PGAM1, Phosphoglycerate mutase 1; PGAM2, Phosphoglycerate mutase 2; Adra1a, adrenergic receptor, alpha 1a; Adra1b, adrenergic receptor, alpha 1b; Adra1d, adrenergic receptor, alpha 1d; Adra2d, adrenergic receptor, alpha 2d; Adrb1, adrenergic receptor, beta 1; Adrb2, adrenergic receptor, beta 2; Adrb3, adrenergic receptor, beta 3; BDNF, brain derived neurotrophic factor; mGluR1, glutamate receptors, metabotropic, 1 (GPCR type); mGluR2, glutamate receptors, metabotropic, 2 (GPCR type); mGluR3, glutamate receptors, metabotropic, 3 (GPCR type); mGluR5, glutamate receptors, metabotropic, 5 (GPCR type); mGluR7, glutamate receptors, metabotropic, 7 (GPCR type); AMPA1, glutamate receptor, ionotropic, alpha-amino-3-hydroxy-5-methyl-4-isoxazolpropionate receptor 1 (ion channel type); AMPA3, glutamate receptor, ionotropic, alpha-amino-3-hydroxy-5-methyl-4-isoxazolpropionate receptor 3 (ion channel type); AMPA4, glutamate receptor, ionotropic, alpha-amino-3-hydroxy-5-methyl-4-isoxazolpropionate receptor 4 (ion channel type); NMDA3A, glutamate receptor, ionotropic, N-methyl-D-aspartate receptor 3A (ion channel type); NMDA3D, glutamate receptor, ionotropic, N-methyl-D-aspartate receptor 3D (ion channel type); CaMKIV, calcium/calmodulin-dependent protein kinase IV; CB1B, cannabinoid receptor 1; ATF4, activating transcription factor 4; PKA, protein kinase A, cAMP dependent catalytic subunit alpha; NR1, glutamate receptor, ionotropic, N-methyl-D-aspartate receptor, subunit zeta-1 (ion channel type); NR2B, glutamate receptor, ionotropic, N-methyl-D-aspartate receptor, subunit epsilon-2 (ion channel type); NCAM, neural cell adhesion molecule 1; MSK, Mitogen and stress activated protein kinase; RasKa, ribosomal protein S6 kinase polypeptide 1; NCX2, solute carrier family 8 (sodium/calcium exchanger), member 2 ; RAS, Harvey rat sarcoma virus oncogene; IL-2, interleukin 2; PP1, protein phosphatase 1; KAR, chloride channel, voltage-sensitive Ka; FOS, FBJ osteosarcoma oncogene; JUN, jun proto-oncogene; MYC, myelocytomatosis oncogene; AC1, adenylate cyclase 1; AC8, adenylate cyclase 8; ERK1/2, mitogen-activated protein kinase; CREB, cAMP responsive element binding protein; TRKB, musculus neurotrophic tyrosine kinase, receptor, type 2; TNF, tumor necrosis factor; EBP, emopamil-binding protein; CN, protein phosphatase 3, catalytic subunit; CaMKII, calcium/calmodulin-dependent protein kinase II; MAPK, mitogen-activated protein kinase; ORL-1, opioid receptor-like 1; Cdk-5, cyclin-dependent kinase 5;

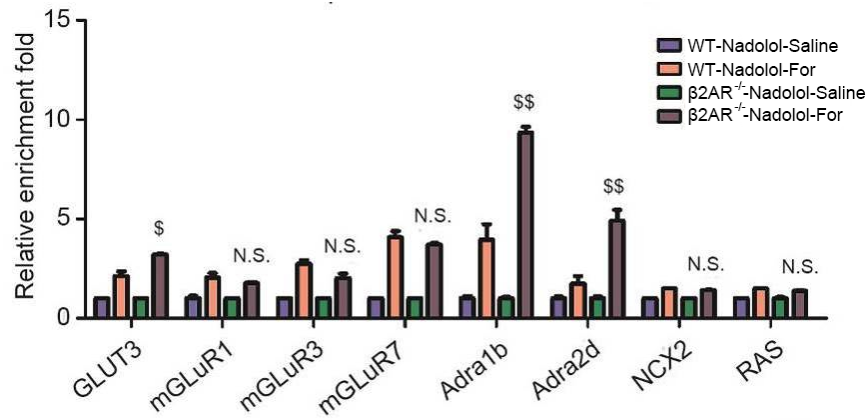


**Fig. S6. Quantitative RT-PCR (QRTPCR) analysis of the mRNA transcription profiles of genes after formoterol stimulation in wild-type or  $\beta 2AR^{-/-}$  mice.**

Data presented show that formoterol induced an mRNA level change independent of the  $\beta 2AR$  activation. Expression levels were normalized to actin levels. Wild-type mice were administered formoterol for 3 days, and the hippocampi were dissected for QRTPCR analysis. A total of 6 mice were used for each group. \$,  $P < 0.05$ ; \$\$,  $P < 0.01$ , the  $\beta 2AR^{-/-}$  mice administered formoterol were compared with the wild-type mice administered formoterol.

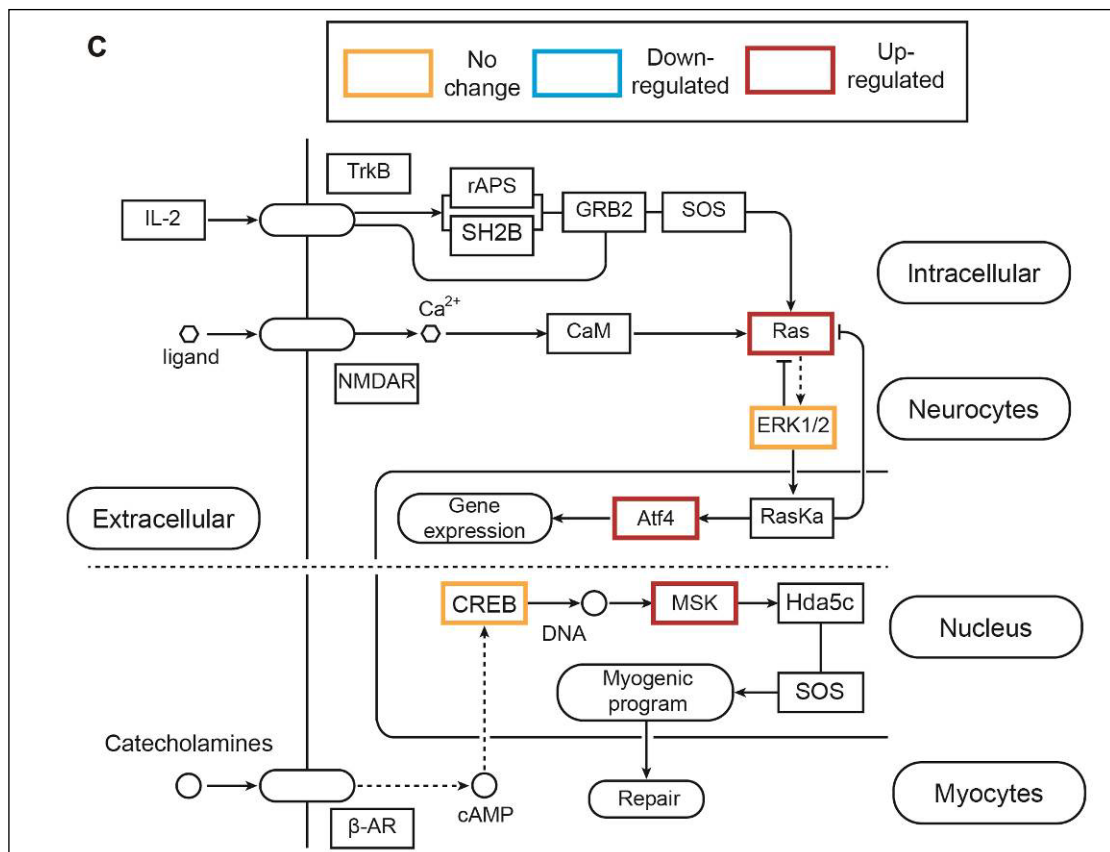
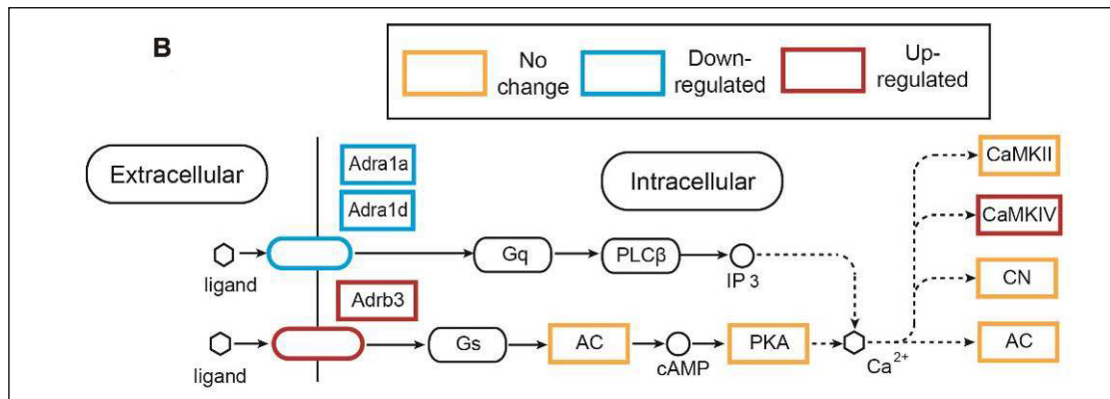
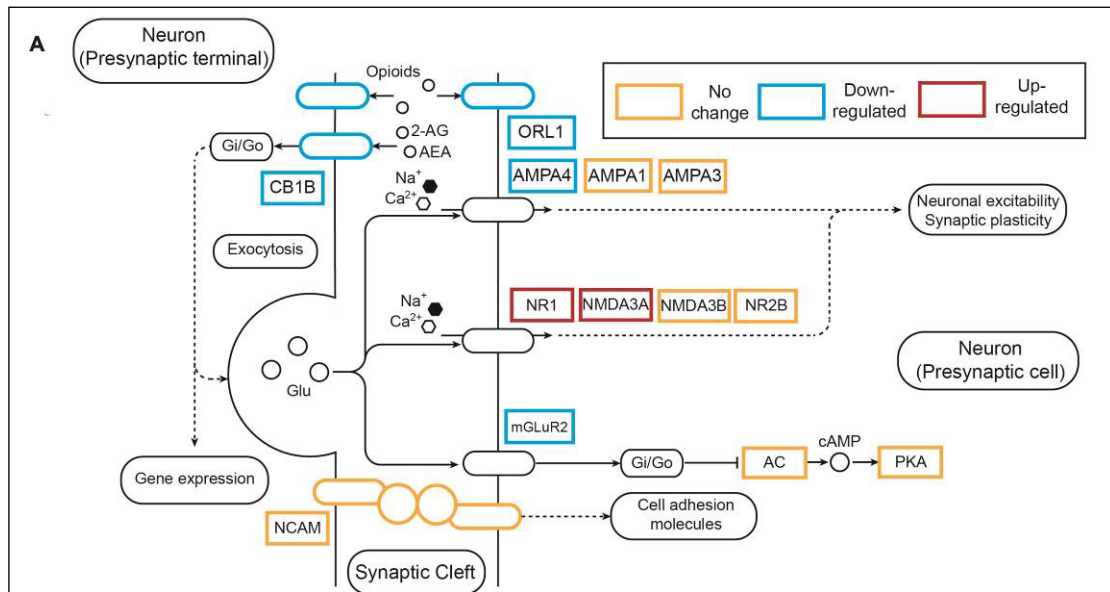




**Fig. S7. Other signaling networks regulated by adaptive  $\beta$ 2AR activation in the hippocampus, derived from QRTPCR results.**

(A) Glutamate receptor-synaptic long term potentiation (LTP) signaling network

(B) Calcium signaling network

(C) Neurotrophic signaling pathway

Red: Activation of  $\beta$ 2AR by formoterol leads to increase of mRNA level of designated gene.

Blue: Activation of  $\beta$ 2AR by formoterol leads to decrease of mRNA level of designated gene.

Yellow: After activation of  $\beta$ 2AR by formoterol, the mRNA level of designated gene was not

changed. Black: The mRNA level of the designated gene was not tested or its change was not dependent on  $\beta$ 2AR.

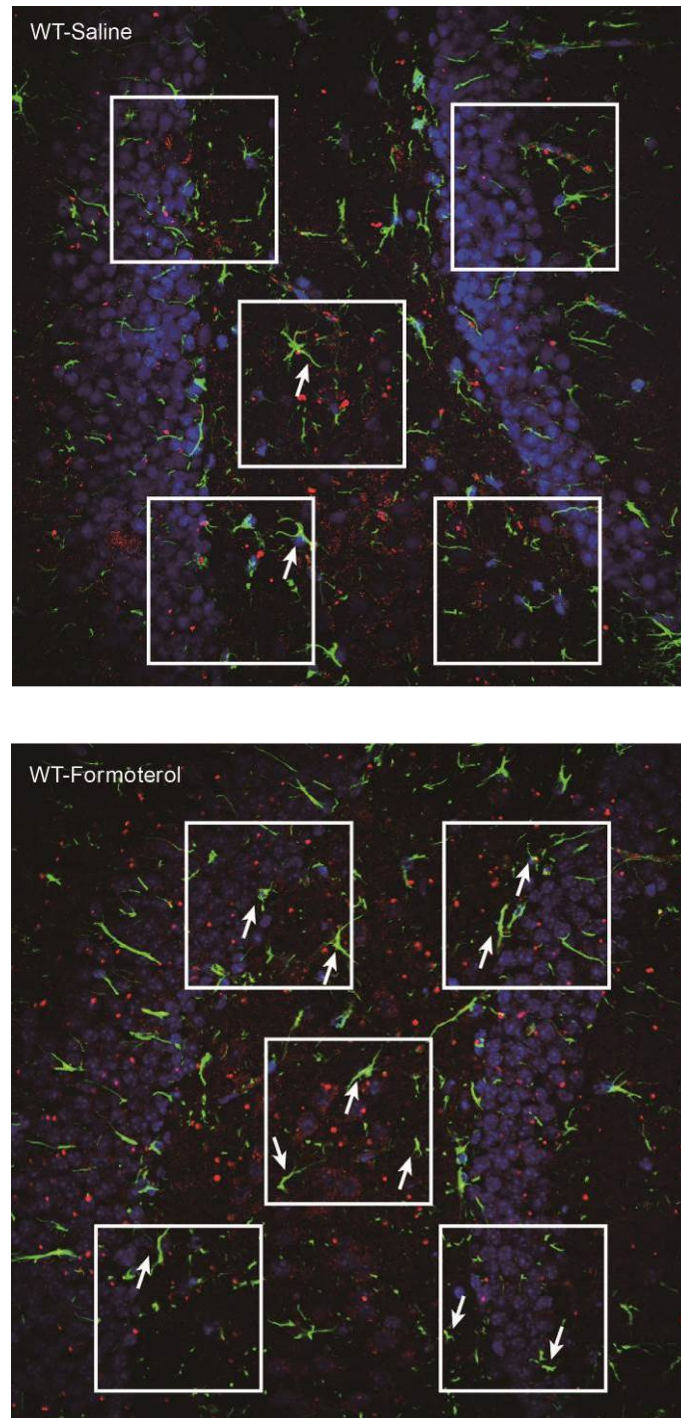


**Fig. S8. Enlarged image of representative immunostaining of MCT4 in hippocampus with/without formoterol treatment for 3 days, related to Fig. 2G.**

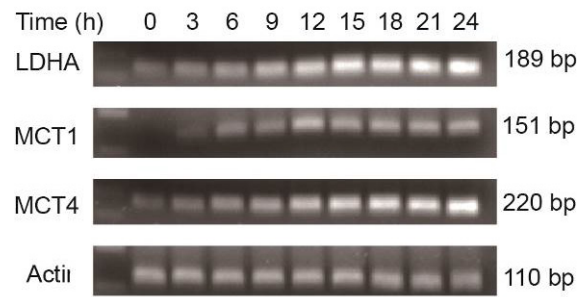


**Fig. S9. Formoterol increased mRNA levels of LDHA, MCT1 and MCT4 in a time dependent manner, related to Fig. 3J.**

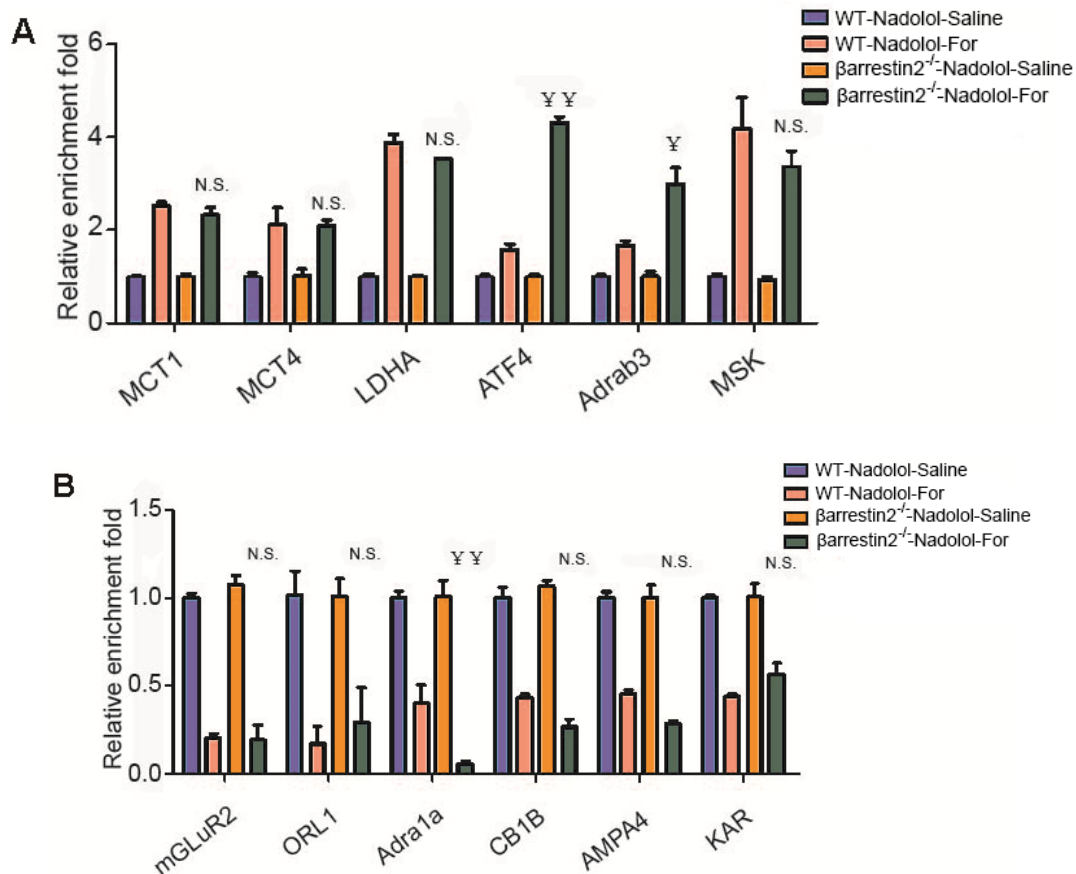


**Fig. S10. Quantitative RT-PCR (QRTPCR) analysis of mRNA transcription profiles of genes after formoterol stimulation in wild type or  $\beta$ -arrestin-2<sup>-/-</sup> mice.**

Data presents that formoterol induced mRNA level change independent of  $\beta$ -arrestin-2 signaling. (A) mRNA level of genes that are increased after formoterol stimulation. (B) mRNA level of genes that are decreased after formoterol stimulation. Expression levels were normalized with actin levels. Wild type mice were administrated formoterol for 3 days and the hippocampus were dissected for QRTPCR analysis. 6 mice were used for each group. ¥,  $P < 0.05$ ; ¥¥,  $P < 0.01$ , the  $\beta$ -arrestin-2<sup>-/-</sup> mice administered formoterol were compared with their wild-type littermates administered formoterol.

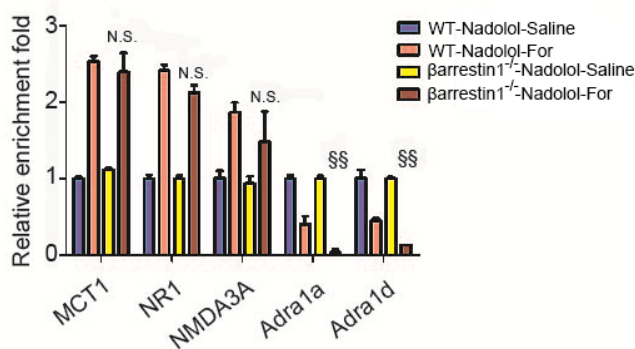


**Fig. S11. Quantitative RT-PCR (QRTPCR) analysis of mRNA transcription profiles of genes after formoterol stimulation in wild type or  $\beta$ -arrestin-1<sup>-/-</sup> mice.**

Data presents that formoterol induced mRNA level change independent of  $\beta$ -arrestin-1 signaling. Expression levels were normalized with actin levels. Wild type mice were administrated formoterol for 3 days and the hippocampus were dissected for QRTPCR analysis. 6 mice were used for each group. \$, P < 0.05, \$\$, P < 0.01, the  $\beta$ -arrestin-1<sup>-/-</sup> mice administered formoterol were compared with their wild-type littermates administered formoterol.

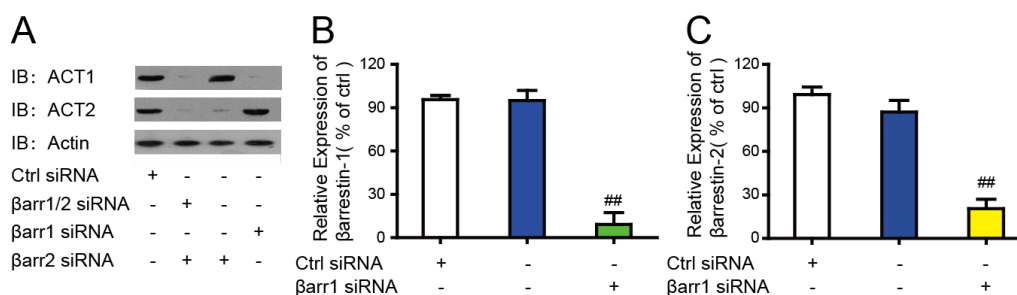


**Fig. S12. Supplemental information for  $\beta$ -arrestin-1 and  $\beta$ -arrestin-2 siRNA knockdown in U251 cells in Figure 5.**

(A) A representative western blot from at least three independent experiments were shown for efficiency of siRNA-mediated knockdown of  $\beta$ arr1 or  $\beta$ arr2 in U251 cells. The  $\beta$ -arrestin-1 has a higher molecular weight than  $\beta$ -arrestin-2. (B) Statistical analysis and bar graph representation of the  $\beta$ arr1 knockdown efficiency in A. (C) Statistical analysis and bar graph representation of the  $\beta$ arr2 knockdown efficiency in A. Data are quantified from at least 3 independent experiments. #, P < 0.05; ##, P < 0.01, cells treated with siRNA were compared with the control cells line (##, P=0.0009, P=0.0019).

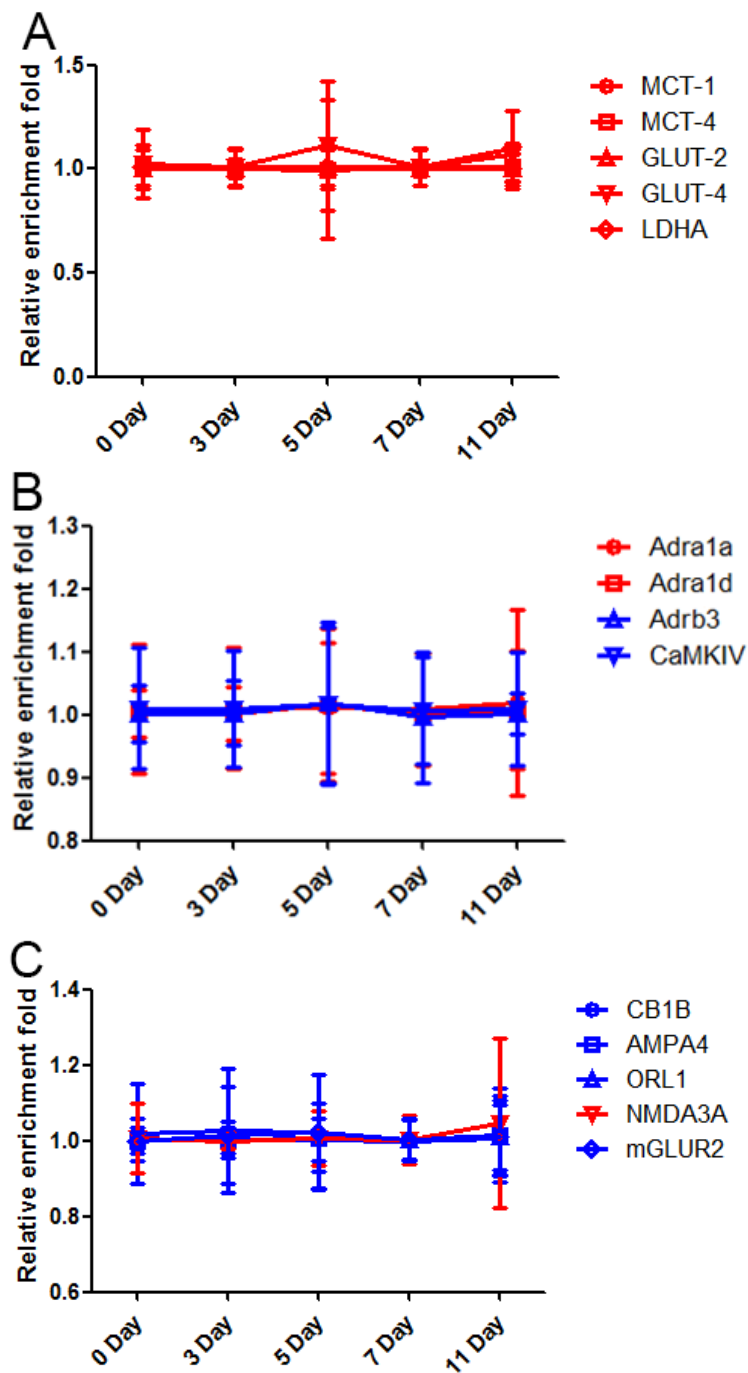


**Fig. S13. Quantitative RT-PCR (QRT-PCR) analysis of mRNA levels of genes important for  $\beta$ 2AR-dependent signaling networks in the hippocampus without formoterol stimulation for 3, 5, 7 or 11 days (Nadolol IP only).**

The results indicated that the examined genes did not change in the control mice during the testing period.

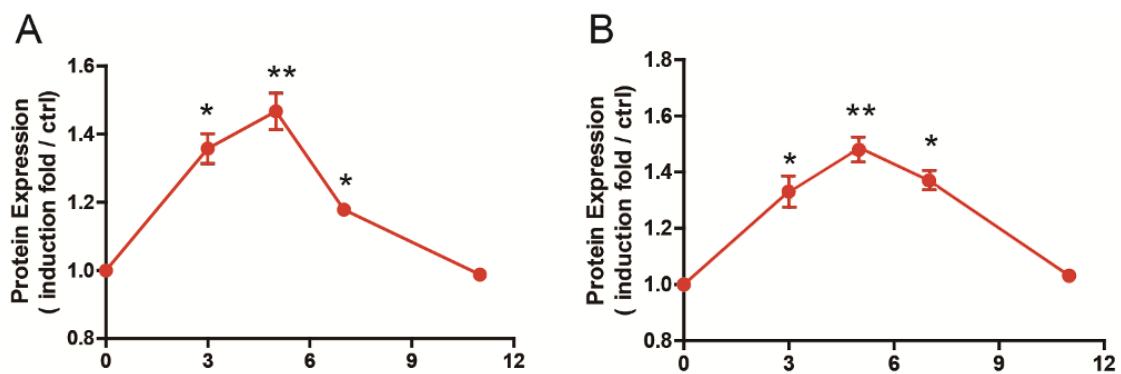


**Fig. S14. Statistical analysis for formoterol induced ERK or CREB phosphorylation in Figure 8G and 8H.**

The C57 wild type mice (n=6 for each group) were administrated formoterol (2 mg/kg) and nadolol (5 mg/kg) as described in Fig. 1A for 3, 5, 7 or 11 days. The ERK or CREB phosphorylation levels in the hippocampus were detected by western with specific antibodies. The statistical analyses were carried out by quantification of the ERK or CREB phosphorylation level and normalized with total ERK or CREB level from Fig. 8G and Fig. 8H. The phospho-ERK and phospho-CREB level were increased from first day to the fifth day, but decreased from fifth day to the eleventh day. \*, P < 0.05; \*\*, P < 0.01; the formoterol administrated mice were compared with the non-administrated animals (Fig. S14A: \*, P=0.0159, P=0.0473, \*\*, P=0.0075; Fig. S14B: \*, P=0.0171, P=0.0176, \*\*, P=0.0092).

## Supplemental Tables

**Table S1. Primer sequences for real time quantitative PCR (QRT-PCR)**

Gene names	Forward	Reverse
MCT4(527/685)	TCAACAAGCGTCGCCCTATT	CACACACACAGCAGTTGAGC
MCT2(843/1000)	CATTCAACCTGCAACCAGCC	ACTCCCCCTCCAGCCATAGT
MCT1(1265/1388)	GCCGGAGTCTTTGGATTTGC	GGCAGCATTCCACAATGGTC
LDHA(926/1025)	CCTGTGTGGAGTGGTGTGAA	TGTGAACCTCCTTCCACTGC
LDHB(833/946)	AAAGGCTACACCAACTGGGC	GCCGTACATTCCCTTCACCA
GLUT1(211/306)	ATGGATCCCAGCAGCAAG	GACACCAGTGTTATAGCCGA
GLUT2(566/663)	CCCTCATCATTGCTGGACGA	GAGTGTGGTTGGAGCGATCT
GLUT3(361/636)	GACAACGAAGGTGACCCCA	CAGTCAGCAGTCCCTCACTTG
GLUT4(233/431)	CGGCTCTGACGATGGGGAA	TTGTGGGATGGAATCCGGTC
PKC-gamma(1184/1307)	TGGAATTGTATGAGGTAATGCTGG	CGCTTCTCTACGAGGGTGC
PKC-alpha(964/1072)	ATCGGACGACTCGGAATGAC	TCGCCCTCTTCTTGTTGAG
HK1(388/487)	GAAGGATGACCAAGTCAAAAA	CATCTCTTTCTTGAAGCGTG
HK2(528/6736)	AGTGCAGAAGGTTGACCAGT	GGTAGCTCCTAGCCCCTTCT
GPI1(281/386)	TGGACTACTCCAAGAACCTT	GAACCACTGAACATGTTGTC
PGK1(1038/1137)	CCAAGACTGGCCAAGCTACT	CCCACAGCCTCGGCATATTT
PGK2(1254/1356)	TGCTCACATGGCTGACCTTG	TAAAGGCCACCTCCAATGGC
PGAM1(496/615)	CATGGTGAGGCCAGGTAAA	AGTAAGGTCTGCGTACCTGC
PGAM2(175/283)	TGTGGCTGGTTTGATGCAGA	CCGACGTGTAGCAGATGTCA
enolas(1217/1367)	GGAAAGGAGTGCTGAAGGCT	TTGGCCCCAACTTGGACTT
Adra1a ( 1103/1221 )	ATGTTAGTCAAAGCATGCACC	GACAGACCAGTTCCTCCTAA
Adra1b(1344/1531)	CACCCTCAGCAGTACCAAGG	GGGGCTTTAGGGTGGAGAAC
Adra1d ( 2057/2151 )	CGAGGTAGAAGCAGTGTCCT	CTCGGAGGTTGCTGTAGTCG C
Adra2a(1227/1395)	GCAACGTGCTGGTTATTATC	CACCACACCTTACCAAAGTA
Adra2b ( 975/1094 )	AGTTCCAGCCTCGGCTAAAAG	TCGGGATCTTCAGGGGTCTC
Adra2d(880/1047)	CCGTCGAGTTCCTTCTGTCTG	AGTACGAACACGCCCATGAC
Adrb1(208/603)	AACCCTGCAACCTGTCTGTCC	CCGTCACACACAGCACATCTA
Adrb2 ( 1409/1297 )	TCACAAAGCCTTCCATGCCT	CAATAGCAACGGCAGAACGG
Adrb3 ( 847/949 )	ATGCCATTTACCCATGGTGC	ACCTGGTGTCTAGGGTTGTGT
BDNF(960/1096)	TCCAAAGGCCAACTGAAGCA	AGGGCCCGAACATACGATTG
mGLuR1(1357/1455)	GATGGGCAGACAGAGATGAA	CATCAAACGACCTGACCTCT
mGLuR2(600/717)	CTACTCTCAGTGATGCTCCC	GCATAGCTGATCTGTGGGAT
mGLuR3(474/574)	GAGACCTTGTTTTAGGGGGCT	CTCCAGGCGTTGGATACCTC
mGLuR5(3332/3465)	GTTGTACCTTCGGATGCCCA	GCCTCCATCCCCTTCTCC
mGLuR7(789/961)	ATCCAGAAGGACACCTCCGA	GGAGCCGTGGATGCATAACT
AMPA1(904/1032)	ATACAGCCGCCGAGAAGAAC	ATTCACAGTCCACCACCACC
AMPA4(683/803)	GGACAACATTGAGACTGCCA	GGAGGTCAAGGTATGCACTG
AMPA3(426/570)	GTTTGTTCATCCAGATGCGCC	GTTTTGCACTGCTGCTTCCA



Gene names	Forward	Reverse
NMDA3A(1344/1436)	GGCTCCTTCCCTACAACCTG	AGCTTGGGGAAGAGAAAGGC
NMDA3B(1204/1322)	AATGACAGCCTTCGGGCTAC	GCCTCTAGGACCTCATGTGC
CaMKIV ( 251/406 )	CAGTACTGAGAACCTCGTCC	TTGAGAGCATAGGGCTTCTG
CB1B(1385/1499)	AGCAAGGACCTGAGACATGC	TGTTATTGGCGTGCTTGTGC
ATF4(1076/1182)	TCGGCCCAAACCTTATGACC	TGGCTGCTGTCTTGTTTTGC
PKA(231/413)	AGCAGGAGAGCGTGAAAGAG	CCAGCTTAACCACTGCAAAA
NR1(488/614)	ACTTCTGTCACCCACAAGCC	TGGGAGTGAAGTGGTCGTTG
NR2B(1305/1393)	TGCTCAACATCATGGAAGAA	CCTGGGGAGTTTCAGGTTCC
NCAM ( 2395/2498 )	AGCTCACTTTGTGTTCAAGGA	CCGCAGAGAAAAGCAATGAG
MSK ( 139/267 )	TGGTGATCATGTCCGAGTTC	CCAGCTTAACCACTGCAAAA
RasKa(253/497)	GCCACATCAAACCTCACTGAC	GTCCTTCCCATCAGCAC
NCX2(1852/1956)	GGTCATTGCTGTTTGTGTGT	ACATAGGCAAAGATGCTCCA
RAS(671/838)	CTGCTCGCACTGTTGAGTCT	TCCGCAATTTATGCTGCCG
IL-2(118/264)	TCAAGCCCCACTTCAAGCTC	CCTGGGGAGTTTCAGGTTCC
PPI ( 1059/1241 )	AAAGAGGCAGTTAGTCACTC	TGCTTTGTGATCATACCCC
KAR(547/744)	ATGTTCCGTCTCCTTGCAG	ACAGGTAAACGCAACTGAGGA
FOS(260/438)	GGCTCTCCTGTCAACACACA	GTCTCCCTCCAGAGCGAAAAA
JUN(1212/1324)	CATCACCCTACACCGACCC	TCTGGCTATGCAGTTCAGCC
MYC(665/859)	CTCCTCGAGCTGTTTGAAGG	TAACCGGCCGCTACAATTC
AC1 ( 764/861 )	TGCTCTTCTTTGGTGTGAAC	CTCAATGCAGTTTCGAGCC
AC8 ( 1902/2029 )	CACTTACCTGCAATACAGCG	AGGTGGCGAAGAGTGTA AAA
ERK1/2 ( 578/726 )	CAAGCTCTTGAAGACACAGC	GATCACAAGTGGTGTTCAGC
CREB ( 11/119 )	ATGACCATGGAATCTGGAGC	CTAATGTGGCAATCTGTGGC C
TRKB ( 1897/2006 )	AGTCGACTACGAGACAAACC	CCGTGGAGGGGATTCATTA
TNF(18/148)	CCGGTGTTTGGCTTTTGGAT	CAGTCTGGAGGTTAGCTGGC
EBP(100/201)	AAGGGTCATTAGCCATGTTGGT	GCTCCAGGTGTGTGAAAGC
CN(691/794)	CAAAGCGCTACTGTTGAGGC	ATTCGGTCTAAGCCCTTGGC
CaMKII(1022/1139)	AGTTCAATGCCAGGAGGAAA	GAAGATTCCTTACACCATCG
MAPK(1076/1248)	CCCAAATGCTGACTCCAAAG	CGTCCAACCTCATGTCAAAC
ORL1-(248/398)	CTAAATGAGACCGTACCCCAT	TGAGGATGACATACATGACG
Cdk5(755/870)	AGCCCTACCCAATGTACCCA	GATGCGCTGCACAGGGTTAC

**Table S2. Primer sequences for the LDHA, MCT1, and MCT4 promoter and HIF-1 $\alpha$  mutations.**

Gene	Oligo names	Forward	Reverse
LDHA	pGL4.16-LDHA-P1 (-3650/-2250)	CAGCCCGACTCACAAAT GGGTTCCCGCACG	CGTGCGGGAACCCATTTG TGAGTCGGGCTG
LDHA	pGL4.16-LDHA-M1 (-2336/-2362)	GTGGGTTCCCGCAAATC CGCCGGCCCCC	GGGGGCCGGCGGATTTGC GGGAACCCAC
LDHA	pGL4.16-LDHA-M2 (-2353/-2348)	CGGGGTACCTCAGGGA AAAAGGCTCTTT	GGGGGCCGGCGGATTTGC GGGAACCCAC
MCT1	pGL4.16-MCT1-P1 (-1201/-6)	CCGCTCGAGGGTAAGT GCAAGAATCAAATTTG	CCCAAGCTTGCACTGCAG TCCGAGG
MCT1	pGL4.16-MCT1-M1 (-1198/-1194)	CCGCTCGAGCTGGCCG CTGACGAGCT	CCCAAGCTTGCACTGCAG TCCGAGGCCAC
MCT1	pGL4.16-MCT1-M2 (-1198/-1194) /(-13/-8)	CCAGCCTGCGCCACCA AAAAACGCACACGCTC GGC	GCCGAGCGTGTGCGTTTT TTGGTGGCGCAGGCTGG
MCT4	pGL4.16-MCT4 (-554/+83)	CCGCTCGAGCGGGACC GGAGAGGAAGC	CCCAAGCTTCCCCGGCCC CAACAGACACAAGAC
MCT4	pGL4.16-MCT4 (-396/+83)	CCGCTCGAGTCGCTGCC CTGGAGGACGTT	CCCAAGCTTCCCCGGCCC CAACAGACACAAGAC
MCT4	pGL4.16-MCT4 (-67/+83)	CCGCTCGAGGCGCCAG CGACCCGAGCACTTA	CCCAAGCTTCCCCGGCCC CAACAGACACAAGAC
HIF-1 $\alpha$	HIF-1 $\alpha$ (S515A)	CACCTGAGCCTAATGAG CCCAGTGAATATTG	CAATATTCCTGGGCTCAT TAGGCTCAGGTG
HIF-1 $\alpha$	HIF-1 $\alpha$ (S515A/TSS385AAA)	AGTTGAATCAGAAGATG AAGAAGAACTCTTTGA CAAACCTT	AAGTTTGTCAAAGAGTTC TTCTTC ATCTTCTGATTCAACT
HIF-1 $\alpha$	HIF-1 $\alpha$ (S515A/T506A)	GTCCTTCCGATGGAAGC GAGAGACAAAGTTCAC CTG	CAGGTGAACCTTGTCTCT CGCTTCCATCGGAAGGAC

**Table S3. Locomotor activity of WT,  $\beta$ 2AR<sup>-/-</sup> and  $\beta$ -arrestin-1<sup>-/-</sup> mice with or without formoterol treatment in the open field**

Genotype	No. of animals	Vertical activity jump, times	Horizontal activity velocity, cm/s	Total distance,cm	Center distance/ total distance,%
WT	20	331.96 ± 40.65	6.94 ± 1.27	2600.35 ± 425.41	7.86 ± 4.18
$\beta$ 2AR <sup>-/-</sup>	10	331.40 ± 40.45	7.01 ± 1.12	2593.16 ± 462.47	8.78 ± 5.93
$\beta$ arrestin-1 <sup>-/-</sup>	10	338.96 ± 50.47	7.23 ± 1.89	2650.68 ± 457.38	8.21 ± 5.68
WT+For	20	334.05 ± 46.19	6.90 ± 1.65	2647.66 ± 411.64	8.46 ± 5.31
WT+DAB	10	342.48 ± 55.37	8.00 ± 2.02	2739.84 ± 474.93	8.93 ± 6.03
WT+DAB+For	10	348.16 ± 27.04	7.55 ± 0.97	2828.60 ± 465.21	7.95 ± 4.07
$\beta$ 2AR <sup>-/-</sup> +For	10	332.80 ± 37.55	7.16 ± 1.38	2583.35 ± 404.38	8.43 ± 5.11
$\beta$ arrestin-1 <sup>-/-</sup> +For	10	339.64 ± 26.54	7.12 ± 1.49	2618.23 ± 411.60	8.26 ± 4.76

Locomotion was tested in a 40 cm × 40 cm open field for 10 min.

**Table S4. Total exploration time of WT,  $\beta$ 2AR<sup>-/-</sup> and  $\beta$ -arrestin-1<sup>-/-</sup> mice in the OR experiments.**

Genotype	No. of animals	Kind of test	Exploration time,s
WT-Nadolol	10	STM	24.02±8.27
	10	LTM	26.06±6.11
$\beta$ 2AR <sup>-/-</sup> -Nadolol	10	STM	23.43±5.12
	10	LTM	26.93±4.38
$\beta$ arrestin-1 <sup>-/-</sup> -Nadolol	10	STM	24.31±6.33
	10	LTM	27.12±6.17
WT-Nadolol-For	10	STM	25.34±6.03
	10	LTM	26.98±5.97
WT-Nadolol-DAB	10	STM	23.14±4.55
	10	LTM	27.02±7.03
WT-Nadolol-DAB-For	10	STM	21.23±9.56
	10	LTM	24.86±8.37
$\beta$ 2AR <sup>-/-</sup> -Nadolol-For	10	STM	23.73±6.03
	10	LTM	27.19±3.24
$\beta$ arrestin-1 <sup>-/-</sup> -Nadolol-For	10	STM	24.55±5.77
	10	LTM	27.32±6.07

OR was tested in a 40 cm × 40 cm open field for 5 min.

## Supplemental Discussion

In addition to the lactate metabolism, the adaptive activation of  $\beta$ 2AR results in multiple signaling network activations; one of the important subnetworks is glutamate receptor mediated LTP (Fig. S7A). Previous studies have demonstrated that emotion enhances learning through norepinephrine (NE)-induced rapid phosphorylation of AMPA receptor (GluR1 subunit), which results in LTP. In these studies, the transient administration of NE stimulated GluR1 phosphorylation within 15 min, but this short-time treatment did not result in changes in protein expression (1). The effect of NE on learning is mainly via  $\beta$ AR, as propranolol totally abolishes its effect. Here, we showed that adaptive  $\beta$ 2AR activation increases NMDA receptor (NR1 subunit) transcription, which is a key hub in LTP formation (2, 3). In addition, the mRNA level of an inhibitor of LTP, the Gi-coupled receptor mGluR2, is decreased after the formoterol-induced adaptive  $\beta$ 2AR activation (Fig. 2A-B and Fig. S7A) (4). The increased expression of NR1 and the decreased expression of mGluR2 are consistent with increased cognitive function after formoterol administration for 3~5 days. Therefore, the previous and our current results provide evidence that  $\beta$ AR signaling could regulate LTP from two different levels. A transient  $\beta$ AR signal modulates the activation of GluR1-LTP by phosphorylation, whereas adaptive  $\beta$ 2AR activation results in the activation of the LTP network through an increase in the expression of key regulators.

Other than glutamate signaling, a cluster of proteins was enriched in the calcium signaling subnetwork (Fig. S7B). Adaptive activation of  $\beta$ 2AR increased the expression levels of CamKIV but decreased the Gq coupled receptor Adra1d ( $\alpha$ 1dAR) and Adra1a ( $\alpha$ 1aAR) (Fig. 2A-B and Fig. S7B). CaMKIV is expressed in restricted tissues, and its expression in the postnatal forebrain is required for memory consolidation and hippocampal late LTP (5). It is particularly required for fear memories through regulating the phospho-CREB levels (6).  $\alpha$ 1aAR and  $\alpha$ 1dAR are receptors for catecholamines and mediate the actions of sympathetic nerves in the brain. Whether changes to these key elements have regional or cell-type specificity and how they correlate to the function of adaptive  $\beta$ 2AR activation await further research.

## Supplemental Methods and Materials

### Reagents

The monoclonal anti-actin antibody (sc-8432) and anti-Histone H3 (sc-398323) antibody, polyclonal anti-CREB antibody (sc-377154), anti-MCT1 antibody (sc14916), anti-MCT4 antibody (sc-50329), anti-GFAP (sc-166481), anti-HIF-1 $\alpha$  (sc-10790) and anti-LDHA antibody (sc-27230) were from Santa Cruz Co. The polyclonal anti-ERK1/2 (4695), anti-phospho-CREB (9198), anti-Flag (2368) and anti-phospho-ERK1/2 (pThr-202, pTyr-204, 4370) antibodies was from Cell Signaling Technology. The metoprolol (M1830000), ICI118, 551(I127), Propranolol (P0884), Epinephrine (4642), Formoterol (F9552), DAB (D8001), H89(B1427) and EZviewäRed Anti-HA Affinity Gel (A2095) were purchased from Sigma (Sigma Aldrich, St Louis, MO, USA). The dual-luciferase reporter assay system (E1960) was from Promega. The NE-PER® Nuclear and Cytoplasmic Extraction Reagents (78835) was from Thermo. The lipofectamine TM2000 (11668-019) was from Invitrogen. The Lactate Assay Kit (ab65331) was from Abcam. All other chemical or reagents were from Sigma unless otherwise specified.

### Animals, Hippocampus Preparation

All animal care protocols and animal experiments were reviewed and approved by the Animal Use Committee of the Shandong University School of Medicine.  $\beta 2AR^{-/-}$ ,  $Arrb1^{-/-}$ , and  $Arrb2^{-/-}$  mice were obtained from Dr. Gang Pei (Tongji University) and Dr. Robert J. Lefkowitz (Duke University, Durham, NC USA) as previously described.  $\beta 1AR^{-/-} / \beta 2AR^{-/-}$  mice were from the Jackson Laboratory (Bar Harbor, ME, USA).  $\beta$ -arrestin 1 $^{-/-}$ ( $Arrb1^{-/-}$ ) ,  $\beta$ -arrestin 2 $^{-/-}$ ( $Arrb2^{-/-}$ ) , and  $\beta 2AR^{-/-}$  mice were maintained and backcrossed to the C57BL/6 mice as described previously (7-9). For  $\beta$ -arrestin 1 $^{-/-}$ ,  $\beta$ -arrestin 2 $^{-/-}$ ,  $\beta 1AR^{-/-}$  and  $\beta 2AR^{-/-}$  mice, their C57BL/6 wild-type littermates were used as the controls. The  $\beta 1AR^{-/-} / \beta 2AR^{-/-}$  double knockout mice were compared with their wild-type littermates ( $\beta 1AR^{+/+} / \beta 2AR^{+/+}$ ), which consisted of a mixed C57/129/DBA/FVB background (8, 10). Mouse genotyping was performed as previously described and further verified by Western blotting after animal experiments (7). For transcriptional profile studies or Western blot analysis, wild-type or specific knockout mice at 8-10 weeks of age were sacrificed by cervical dislocation after certain training procedures. The hippocampus was obtained as previously described with microscissors and either lysed with Trizol for RT-PCR or lysed with RIPA buffer for Western

blotting (11).

### **Primary Astrocyte Cell Culture**

The primary astrocyte cell culture for  $\beta 2AR^{-/-}$  mice,  $\beta 1AR^{-/-}/\beta 2AR^{-/-}$  double knockout mice or  $\beta$ -arrestin 1 $^{-/-}$  (*Arrb1 $^{-/-}$* ) mice and their wild-type littermates were performed as previously described (12-14). Four P1 (postnatal day1) mouse pup cerebral cortices were dissected to prepare astrocyte enriched cultures in one poly-D-lysine (50  $\mu$ g/ml) coated T75 tissue culture flask. Briefly, cortex pieces were put into 50 ml Falcon tube and added with 10 times volume of 0.25% trypsin, incubated at 37°C for 30 min, with shaking every 10 min. The supernatant was decanted and the tissue pellet was dissociated into 10 ml astrocyte plating medium with vigorous pipetting (20 to 30 times). The dissociated single cell suspension was transferred into a T75 culture flask and the microglia and the oligodendrocyte precursor cells (OPC) were removed by further cell culture as previously described. The whole cell culture procedure took 14-18 days, and the purity of astrocyte cells was examined by GFAP staining.

### **Cell Culture Conditions and Treatments**

U251 astrocyte cells were purchased from the American Type Culture Collection (ATCC) (Maryland, USA) and cultured at 37°C and 5% CO<sub>2</sub> in DMEM media, supplemented with 10% heat inactivated fetal bovine serum (Hyclone Thermo Scientific, Scoresby, Victoria, Australia, FBS), 100 U/ml penicillin and 100  $\mu$ g/ml streptomycin. The primary astrocyte cells were cultured in the same medium as U251 after purification. U251 cells or primary astrocyte cells were starved for 8 h in DMEM media before treatment with agonists or antagonists. For chemical treatment, epinephrine (EPI) and formoterol were freshly dissolved in PBS buffer (or DMSO) to prepare a stock solution and were then diluted to medium, supplemented with 1 mmol/l ascorbic acid to decrease oxidation. H89 was dissolved in PBS buffer, and the U0126 and the ICI118,551 were dissolved in DMSO and applied to the medium with a final concentration of 10  $\mu$ mol/l. EPI and formoterol were immediately administered to the cell culture. The specific antagonists or inhibitors, including U0126, H89 and ICI118,551, were pre-incubated with cells for 30 min before agonist stimulation. For all experiments, the cells were exposed to these chemicals the whole time before being harvested.

### **Morris Water Maze (MWM) Experiments**

All behavior experiments were performed blind to genotypes. For each day, before formoterol treatment, 5 mg/kg nadolol was administered to prevent the effects of formoterol in the

peripheral tissues. Thirty min after nadolol administration, the mice were randomly separated into two groups and were injected with one of five doses of formoterol (0.5, 1, 2, 4 or 8 mg/kg) or saline. The protocol was designed according to the pharmacokinetics of formoterol, which has a half-life of approximately 10 h and remains in the brain for over 24 h. The MWM experiments were performed in an apparatus with 80 cm diameter and stainless steel edges painted flat black. The water tank was surrounded by removable curtains to either conceal or reveal room cues. The three walls closest to the maze (designated as North, South, East and West) had geometric figures fixed onto them. A platform (3 × 3 cm) was 1–2 cm below the water surface and was masked by being transparent against a black background. A camera was mounted above the maze and connected to a computer. The mice movements were recorded and analyzed by Polytrack software (Polytrack software, San Diego Instruments, San Diego, CA). All experiments were conducted at a water temperature of 21±1°C. Spatial learning and reference memory tests were conducted in three phases: acquisition, reversal, and cued. The first two phases consisted of four trials/day for 5, 7, or 12 days with the curtains opened and with the submerged platform. This was followed by an extra day when a single probe trial was given with the removed platform. The acquisition phase began 5, 7, or 12 days after straight channel testing.  $\beta 2AR^{-/-}$  mice or their wild-type littermates were started at one of four positions located distal to the quadrant containing the platform in a quasi-random order with the restraint that they received one trial from each starting position/day. One min was allowed for each mouse to locate the platform. If the animal did not find the platform during the 1 min limit, it was led by the experimenter to the platform resting for 1 min. The latency to escape the water and to locate the hidden platform for each mouse was recorded and analyzed. On the day after the last acquisition trial, each mouse was given a 60 s probe trial with the platform removed. The mice were allowed to swim freely in the pool for 60 s, the time spent in each quadrant and the crossing numbers on the correct platform location were recorded and analyzed by Polytrack software (Polytrack software, San Diego Instruments, San Diego, CA).

### **Object Recognition Task**

For adaptive  $\beta 2AR$  activation, the mice were continuously administered formoterol/nadolol as described in the MWM experiments for 3 days before the object recognition task. For the inhibition of glycogen phosphorylation with 1,4-dideoxy-1,4-imino-D-arabinitol (DAB), either vehicle or 300  $\mu\text{M}$  (300 pmol) DAB were bilaterally injected in mice 24 h before the recognition task. The object recognition task was performed by revising the procedures from



Clarke (15) and Liu (16). The  $\beta 2AR^{-/-}$  mice or their wild-type littermates were first placed in an empty open field box (45x45x30 cm) made of wood and painted black inside. The mice were habituated to the task for 10 min. No data were recorded for habituation. The mice were conducted for sample phase 24 h later, where they were exposed to two identical objects (O1a and O1b) located in the left and right corners for 5 min. The objects were placed approximately 10 cm distant from two corners of the box. Care was taken to avoid olfactory stimuli by carefully cleaning the objects. Mice were permitted to freely explore the objects until they spent a total of 5 min on object exploration (the exploration was operationally defined as directing the nose to the object at a distance of less than 2 cm and/or touching the front paw to the object). The time that each mouse spent with each object was recorded. The mice were returned to their home cage thereafter and injected the formoterol/nadolol or vehicle/nadolol (2 mg/kg). After a delay of 3 h (Short Term Memory) or 24 h (Long Term Memory), the  $\beta 2AR^{-/-}$  mice or their wild-type littermates were placed back in the setup (recall trial) and then presented with one of the familiar objects (O1) and a novel object (O2) for a further 5 min. The time (t) spent (in seconds) exploring the objects (O1 and O2) was recorded. The discrimination ratio (DR) was calculated using the formula [new familiar time (O2) / total exploration time] x100. Test phase data are presented as the discrimination index (DI), calculated as [(new familiar time – old familiar time)/total exploration time] x100 as previously described (17). A greater DR or DI suggests a greater preference for exploring the new object.

### **Quantitative Real-Time PCR**

Total RNA from the mouse hippocampus, primary astrocyte cells or U251 cells were extracted using a standard TRIzol RNA isolation method (Invitrogen) as previously described (7). The reverse transcription to cDNA and PCR experiments were performed with the Revertra Ace qPCR RT Kit (TOYOBO FEQ-101) using 0.5  $\mu$ g for each sample, according to the manufacturer's protocols. The quantitative Real-time PCR was conducted in the LightCycler apparatus (BIO-RAD) using the FastStart Universal SYBR Green Master (Roche). qPCR protocol is following: 95°C, 10 min, then 40 cycles of 95°C, 15 s; 60°C, 1 min; following with increasing the temperature from 65°C to 95°C and kept the speed as 0.1°C/s. The expression value was normalized to GAPDH or  $\beta$ -actin in the same sample and then compared with the control. The sequences of the primer pairs are provided in Supplemental Table S1.

### **Lactate Level Measurement**

After the mice were sacrificed, the hippocampus was dissected, washed with PBS, frozen and thawed three times, and then lysed by a dounce homogenizer in cold water. The primary astrocyte cells or U251 cells were washed twice with PBS and maintained in DMEM (glucose, pyruvate, and serum free) for 30 min. The cells were administered control vehicle or chemicals for varied concentrations or times. The cells were then washed twice with cold PBS, once with cold water and finally lysed in cold water ( $6 \times 10^5$  cells/ 200  $\mu$ L). The lactate levels were measured with the Lactate Assay Kit (abcam; ab65331) following the manufacturer's instructions.

### **Constructs**

The LDHA, MCT1 and MCT4 promoters were amplified by PCRs of mouse genomic DNA using primers indicated in Supplemental Table S2. The PCR amplified products containing SacI or BamHI (5-end), and HindIII (3-end) restriction sites were ligated to the pGL4.16 basic vector (Promega); the plasmid sequence were confirmed by DNA sequencing. The  $\beta$ -arrestin-1-YFP,  $\beta$ -arrestin-2-RFP, Flag- $\beta$ -arrestin-1 and Flag- $\beta$ -arrestin-2 plasmids are generous gifts from the Dr. Lefkowitz lab at Duke University. The HA-HIF-1 $\alpha$  plasmid was purchased from Addgene (#18949) (18).

### **Site-Directed Mutagenesis**

The HA-HIF-1 $\alpha$  mutants (S515A, S515A/TSS385AAA and S515A/T506A) and promoter truncations or mutations (LDHA-M1, LDHA-M2, MCT1-M1 and MCT1-M2) were generated using the QuickChange mutagenesis kit obtained from Stratagene. All mutations, truncations or deletions were verified by DNA sequencing (19). All primers are listed in Supplemental Table S2.

### **Plasmid Transfection, Immunoprecipitation and Western Blotting**

For exogenously introduced transcriptional factors including *Creb*, HIF-1 $\alpha$  and different HIF-1 $\alpha$  mutants, a total of 6  $\mu$ g plasmids were transfected to a 10 cm dish of U251 cells by lipofectamine 2000 (Invitrogen). To monitor protein expression levels, cells were collected 48-72 h post-transfection with lysis buffer (50 mM Tris, pH 8.0; 150 mM NaCl; 1 mM NaF; 1% NP-40; 2 mM EDTA; Tris-HCl, pH 8.0; 10% glycerol; 0.25% sodium deoxycholate; 1 mM Na<sub>3</sub>VO<sub>4</sub>; 0.3  $\mu$ M Aprotinin; 130  $\mu$ M Bestatin; 1  $\mu$ M Leupeptin; 1  $\mu$ M Repstatin; and 0.5% IAA). Cell lysates were subjected to end-to-end rotation for 20 min and spun at 12,000

rpm for 20 min at 4°C. Then, an equal volume of 2× loading buffer was added. Proteins were denatured in loading buffer and subjected to Western blot analysis. The protein bands from Western blots were quantified with ImageJ software (National Institutes of Health, Bethesda MD).

For immunoprecipitation, plasmids encoding HA-HIF-1 $\alpha$ , Flag- $\beta$ -arrestin-1, Flag- $\beta$ -arrestin-2 and control pCDNA3.1 were transfected or co-transfected into U251 cells that were cultured in 150-mm dishes. After allowing 30 h of protein expression, the cells were switched to 4 mL PBS buffer with calcium and magnesium, supplemented with HEPES (pH=7.5) to a final concentration of 20 mM. After exposure of the cells to formoterol for 1 h, the stimulation was stopped by the addition of 2 mM dithiobis[succinimidylpropionate] (DSP), and the plates were rocked slowly for 30 min at room temperature. The cells were then added to 1 M Tris to terminate the DSP reaction. The cells were then washed 2-3 times with cold PBS plus 20 mM Hepes (pH 7.5) and subjected to the lysis buffer (50 mM Tris, pH 7.4; 150 mM NaCl; 1% NP-40; 0.5% sodium deoxycholate; 2 mM sodium pyrophosphate; 5 mM NaF; 25 mM  $\beta$ -glycerophosphate; 1 mM EDTA; and 1 mM Na<sub>3</sub>VO<sub>4</sub> supplemented with protease inhibitor cocktail [Roche, Basel Switzerland]) for 1 h. The cell lysates were then incubated with HA-beads for 4-6 hours and the HIF-1 $\alpha$  complex was isolated by precipitation and subjected to Western blot analysis. The Western blotting was analyzed as previously described (20).

### siRNA Transfection

Lipofectamine 2000 was used for siRNA transfection in U251 cells according to the manufacturer's instructions. The siRNA sequences are:  $\beta$ -arrestin1, 5'-GAAGUCAAGCCUUCUGCGCGGAGA-3') and  $\beta$ -arrestin2, 5'-CCUGAAGGACCGCAAAGUGUUUGUG-3'.

### Luciferase Reporter Assay

U251 cells were cultured to 70-80% confluence for transfection experiments in 24-well plates. The cells were co-transfected with the specific pGL4.16-target promoter luciferase plasmids (wild type or different truncations or mutants) or control pGL4.16-empty plasmids, transcriptional factor expression plasmids (CREB or HIF-1 $\alpha$ ) and pRL-TK renilla plasmid using Lipofectamine 2000 (Invitrogen). After transfection for 36 h, the cells were treated with suitable stimulators and the luciferase activities were measured using the dual-luciferase

reporter assay system (Promega) as previously described (7). The level of renilla luciferase activity was used as a reference, and the results are represented as the average of at least triplicate experiments.

### **Immunofluorescence**

The immunofluorescence was performed as previously described (VLGR1 JBC paper). The U251 or primary astrocytes were washed in PBS and then fixed 20 min in 4% paraformaldehyde at room temperature. Fixed cells were washed with PBS and nonspecific immune-reacting sites were blocked with 0.5% BSA for 1 h at room temperature. Cells were incubated overnight at 4°C in freshly prepared HIF-1 $\alpha$ ; arrestin1, arrestin2 or phospho-ERK antibody. After carefully rinsing with PBS, cells were incubated in a solution containing donkey Cy3-conjugated anti-rabbit Igs for 1 h at room temperature (1:500 dilution). After washed again in PBS, cells were incubated in a DAPI solution in water for 1 min. The cells were washed again with PBS and the immunofluorescence was performed using a laser-scanning confocal microscope (Leica, Germany). For immunofluorescence in the hippocampus, the mice were decapitated and the brains were removed immediately. The brains were embedded with the O.C.T ( SAKURA) on the dry ice, then 6- $\mu$ m-thick coronal serial sections were cut at the level of hippocampus and mounted on poly-L-lysine-coated slides. Brain slides incubated in the ice-cold acetone at 4°C within 30 min and then washed them with the PBS. The slides were incubated in the citrate buffer solution for the antigen retrieval. Non-specific binding sites were blocked with 2.5% (wt/vol) BSA, 1% (vol/vol) donkey serum and 0.1% (vol/vol) Triton-X100 in PBS for 1 h. After blocking, slides were incubated in GFAP fluorescent antibody (1:500, eBioscience) and primary antibody against MCT4 (1:25, Santacruz) at 4°C overnight. Subsequently, slides were incubated for 1.5 h with the 568 donkey anti-rabbit IgG (H+L) (1:500, Invitrogen) at the room temperature for 2 h. For nuclear staining, the slides were incubated with DAPI (1:2000, Beyotime) for 15 min at the room temperature. The immunofluorescence results were examined with the LSM 780 laser confocal fluorescence microscope (Carl Zeiss). The normal saline group was treated as control. Data in the graphs are presented as the mean  $\pm$  SEM.

### **Nucleus Proteins Extract**

Cells were washed twice with phosphate-buffered saline (PBS) (Ca<sup>2+</sup> and Mg<sup>2+</sup>-free) and re-suspended in solution A (10 mM HEPES, pH 7.9, 10 mM KCl, 1.5 mM MgCl<sub>2</sub>, 0.34 M sucrose, 10% glycerol, 1 mM dithiothreitol, 10 mM NaF, 1 mM Na<sub>2</sub>VO<sub>3</sub>, protease inhibitors

(Roche)). To extract the nucleus fractions, lysates were added by Triton X-100 with a final concentration of 0.1%. Cytosolic proteins (S1) were separated from nuclei by centrifugation (4 min, 1,300x g). The pellet (nuclei fraction) was washed once in solution A, and then lysed in solution B (20 mM HEPES, pH 7.9, 420 mM NaCl, 1.5 mM MgCl<sub>2</sub>, 25% glycerol, 3 mM EDTA, 0.2 mM EGTA, 1 mM dithiothreitol and protease inhibitors) for 30 min. The lysates were then centrifuged (4 min, 1,700 x g), to remove insoluble chromatin.

### **Whole-Cell [3H]-CGP12177A Binding Assay**

The hippocampus was first isolated from the injected mice, and the primary cells were then purified according to a previously published procedure (21). The cells were pre-incubated with PBS (Saline), the specific  $\beta$ 1AR antagonist CGP-20712A (10  $\mu$ M), or the specific  $\beta$ 2AR antagonist ICI-118,551 (10  $\mu$ M) at 37°C for 30 min (22). The cells were then incubated with [3H]-CGP-12177A (100 nM) for 3 h with constant shaking at 37°C. Following washing with PBS 3 times, the cells were lysed, and the radio-activities of the radioligand binding to the cell surface were measured using a liquid scintillation counter.

### **Signaling Clustering Analysis**

We obtained all of the signaling pathways related to learning and memory, synapse plasticity and metabolism from the KEGG pathway database (<http://www.genome.jp/kegg>). We then used the DAVID website to perform KEGG pathway cluster analysis of changed genes after formoterol administration (23). Bioinformatics enrichment tools: paths toward the comprehensive functional analysis of large gene lists (24). The only pathway that contained more than two genes with  $P < 1.0E-03$  was regarded as signaling network change after formoterol treatment.

### **Statistics**

All data are presented as the mean  $\pm$  SD from at least three independent experiments. Statistical comparisons were performed with ANOVA tests using GraphPad Prism5. Significant differences were designated as follows: \*, #, \$,  $P < 0.05$ ; \*\*, ##, \$\$,  $P < 0.01$ ; \*\*\*, ###, \$\$\$,  $P < 0.005$ . The sequence alignments were performed using T-coffee.

**Supplemental References**

1. Hu H, Real E, Takamiya K, Kang MG, Ledoux J, Huganir RL, et al. (2007): Emotion enhances learning via norepinephrine regulation of AMPA-receptor trafficking. *Cell*. 131:160-173.
2. Dang MT, Yokoi F, Yin HH, Lovinger DM, Wang Y, Li Y (2006): Disrupted motor learning and long-term synaptic plasticity in mice lacking NMDAR1 in the striatum. *Proceedings of the National Academy of Sciences of the United States of America*. 103:15254-15259.
3. Pinheiro PS, Mulle C (2008): Presynaptic glutamate receptors: physiological functions and mechanisms of action. *Nat Rev Neurosci*. 9:423-436.
4. Nicholls RE, Zhang XL, Bailey CP, Conklin BR, Kandel ER, Stanton PK (2006): mGluR2 acts through inhibitory Galpha subunits to regulate transmission and long-term plasticity at hippocampal mossy fiber-CA3 synapses. *Proceedings of the National Academy of Sciences of the United States of America*. 103:6380-6385.
5. Kang H, Sun LD, Atkins CM, Soderling TR, Wilson MA, Tonegawa S (2001): An important role of neural activity-dependent CaMKIV signaling in the consolidation of long-term memory. *Cell*. 106:771-783.
6. Wei F, Qiu CS, Liauw J, Robinson DA, Ho N, Chatila T, et al. (2002): Calcium-calmodulin-dependent protein kinase IV is required for fear memory. *Nat Neurosci*. 5:573-579.
7. Wang HM, Dong JH, Li Q, Hu Q, Ning SL, Zheng W, et al. (2014): A stress response pathway in mice upregulates somatostatin level and transcription in pancreatic delta cells through Gs and beta-arrestin 1. *Diabetologia*. 57:1899-1910.
8. Bernstein D, Fajardo G, Zhao M, Urashima T, Powers J, Berry G, et al. (2005): Differential cardioprotective/cardiotoxic effects mediated by beta-adrenergic receptor subtypes. *Am J Physiol Heart Circ Physiol*. 289:H2441-2449.
9. Hara MR, Kovacs JJ, Whalen EJ, Rajagopal S, Strachan RT, Grant W, et al. (2011): A stress response pathway regulates DNA damage through beta2-adrenoreceptors and beta-arrestin-1. *Nature*. 477:349-353.
10. Rohrer DK, Chruscinski A, Schauble EH, Bernstein D, Kobilka BK (1999): Cardiovascular and metabolic alterations in mice lacking both beta1- and beta2-adrenergic receptors. *J Biol Chem*. 274:16701-16708.
11. Lins BR, Ballendine SA, Howland JG (2014): Altered object exploration but not temporal order memory retrieval in an object recognition test following treatment of rats with the group II metabotropic glutamate receptor agonist LY379268. *Neurosci Lett*. 560:41-45.
12. Sorg O, Magistretti PJ (1992): Vasoactive intestinal peptide and noradrenaline exert long-term control on glycogen levels in astrocytes: blockade by protein synthesis inhibition. *The Journal of neuroscience : the official journal of the Society for*

*Neuroscience*. 12:4923-4931.

13. Armstrong RC (1998): Isolation and characterization of immature oligodendrocyte lineage cells. *Methods*. 16:282-292.
14. Siao CJ, Tsirka SE (2002): Tissue plasminogen activator mediates microglial activation via its finger domain through annexin II. *The Journal of neuroscience : the official journal of the Society for Neuroscience*. 22:3352-3358.
15. Clarke JR, Cammarota M, Gruart A, Izquierdo I, Delgado-Garcia JM (2010): Plastic modifications induced by object recognition memory processing. *Proceedings of the National Academy of Sciences of the United States of America*. 107:2652-2657.
16. Liu X, Ma L, Li HH, Huang B, Li YX, Tao YZ, et al. (2015): beta-Arrestin-biased signaling mediates memory reconsolidation. *Proceedings of the National Academy of Sciences of the United States of America*. 112:4483-4488.
17. Lins BR, Ballendine SA, Howland JG (2014): Altered object exploration but not temporal order memory retrieval in an object recognition test following treatment of rats with the group II metabotropic glutamate receptor agonist LY379268. *Neurosci Lett*. 560:41-45.
18. Kondo K, Klco J, Nakamura E, Lechpammer M, Kaelin WG, Jr. (2002): Inhibition of HIF is necessary for tumor suppression by the von Hippel-Lindau protein. *Cancer cell*. 1:237-246.
19. Pan C, Liu HD, Gong Z, Yu X, Hou XB, Xie DD, et al. (2013): Cadmium is a potent inhibitor of PPM phosphatases and targets the M1 binding site. *Scientific reports*. 3:2333.
20. Wang HM, Xu YF, Ning SL, Yang DX, Li Y, Du YJ, et al. (2014): The catalytic region and PEST domain of PTPN18 distinctly regulate the HER2 phosphorylation and ubiquitination barcodes. *Cell research*. 24:1067-1090.
21. Gibbs ME, Hutchinson DS, Summers RJ (2010): Noradrenaline release in the locus coeruleus modulates memory formation and consolidation; roles for alpha- and beta-adrenergic receptors. *Neuroscience*. 170:1209-1222.
22. Catus SL, Gibbs ME, Sato M, Summers RJ, Hutchinson DS (2011): Role of beta-adrenoceptors in glucose uptake in astrocytes using beta-adrenoceptor knockout mice. *British journal of pharmacology*. 162:1700-1715.
23. Huang da W, Sherman BT, Lempicki RA (2009): Systematic and integrative analysis of large gene lists using DAVID bioinformatics resources. *Nature protocols*. 4:44-57.
24. Huang da W, Sherman BT, Lempicki RA (2009): Bioinformatics enrichment tools: paths toward the comprehensive functional analysis of large gene lists. *Nucleic acids research*. 37:1-13.